Synthesis of Carbon Nanomaterials in Flames

Z.A. Mansurov

Institute of Combustion Problems, 172 Bogenbai Batyr St.,
050012 Almaty, Republic of Kazakhstan

Abstract

Usage of combustion processes for production of target products is less common than the application of catalytic processes. However, there are known examples of production of carbon black, HCl, TiO_2 etc. Some research work was done at the Institute of Combustion Problems (Almaty, Kazakhstan) consider the synthesis in flame of carbon nanomaterials: fullerenes, nanotubes and soot nanobeads with superhydrophobic surface. An alternative of fullerenes and nanotubes synthesis in arc discharge of graphite is the method using stationary hydrocarbon flames. Flame is a self-sustaining system in which the hydrocarbons can be precursors of carbon nanomaterials, and the heat released during combustion, is a parameters of the process control. It is known that PAH are nucleation centers of forming soot i.e. PAH can be converted into either soot or fullerenes. The formation of CNTs occurs in diffusion flames from the fuel side and is initiated by transition metals particles. The paper presents data on the formation of fullerenes and carbon nanotubes as well as soot with the superhydrophobic surface, obtained on nickel and silicon supports in benzene-oxygen and propane-oxygen diffusion flames. New results regarding the synthesis of superhydrophobic surface with a contact angle 135-175° have great practical interest as anti-corrosion additives to various materials.

Fullerenes and Their Formation in the Combustion Regime

The discovery of fullerenes representing a new form of existence of one of the most abundant elements on the Earth - carbon - has been recognized as one of the most significant achievements in the science of the XX century. Despite the fact that it has long been known that the carbon atoms are unique in their ability to bind into complex three-dimensional branched structures, which forms the basis for the whole organic chemistry, the possibility of formation of stable carcass molecules from only one carbon was, nevertheless, unexpected.

The fullerenes C_{60} and C_{70} were identified in 1985 [1] and obtained in macroscopic amounts in 1990 in the process of evaporation of graphite by an arc discharge. The C_{60} and C_{70} fullerene ions were detected in flames in 1987 and identified by the mass-spectrometry method [2-4]. Howard et al. [5, 6] have obtained large amounts of C_{60} and C_{70} in laminar premixed soot forming flames of benzene and oxygen at low pressures. The largest amount of $C_{60} + C_{700}$ comprising 20% of the soot obtained, was detected at a pressure of 69 torr, a ratio C/O = 0.989, and a 25% helium content. Unlike the evaporation of graphite, in the fullerenes formed in flames the ratio C_{70}/C_{60} changes from 0.26 to 8.8 (in the case of evaporation of graphite, this ratio changes from 0.02 to 0.18).

All fullerenes fall into the class of carbons with a polyhedral closed shell. They were detected as ionized particles in the fuel-rich plane premixed acetylene and benzene-oxygen flames at low pressures with use of the molecular-beam sampling in combination with the mass-spectrometry analysis [3].

More recently, macroscopic amounts of not only of the C_{60} and C_{70} fullerenes [4], but also more large ones, such as - C_{116} [6], were extracted with use of soot solvents from the low-pressure laminar premixed benzene flames.

The reactions of formation of fullerenes and soot in an arc discharge can have much in common with reactions occurring in the fuel-rich flames. The bulb-like fullerene nanostructures, formed hand in hand with fullerenes and soot, were detected in soot with use of the high-resolution transmission electron microscopy [7].

Figure 1 presents the concentration profiles of the fullerenes and soot formed in a benzene/oxygen/

*corresponding author. E-mail: Zmansurov@ kaznu.kz

 Printed in Kazakhstan

argon flame with C/O = 0.88 and its temperature profile. As is seen, the fullerenes are formed after the main stage of the soot formation. When the ratio C/O increases from 0.88 to 0.96, the concentration profile of the fullerenes becomes monotonically increasing [8].

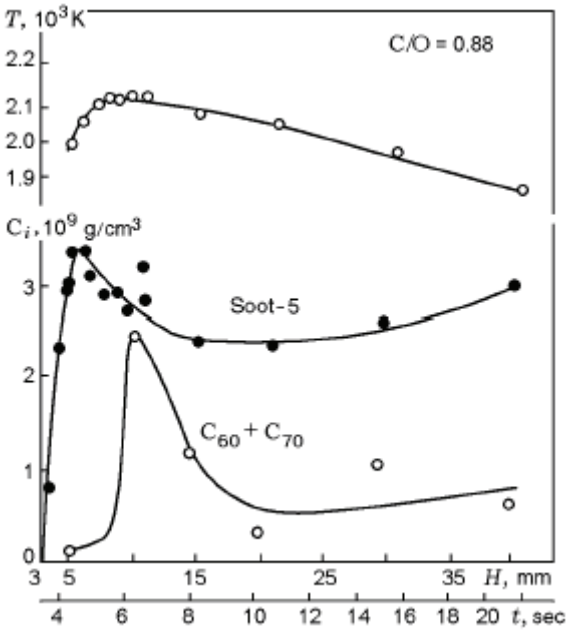

Fig.1. Concentration profiles of the fullerenes and soot and the temperature profile in a benzene/oxygen/argon flame [8]

It has been established that, at the front of a flame, the number of the structures with a closed shell in the soot as well as the concentration of the fullerene molecules in the gas phase increase with increase in the time of their stay in this region. In the region located at a height of 70 mm above a burner the concentrations of the fullerenes and the structures with a closed shell were lower than those in the regions located at a height of 60 and 120 mm. The highly ordered nanostructures, such as nanotubes and fullerene bulbs, were detected in solid samples taken from the walls and the upper part of the combustion chamber, which points to the fact that they are formed in the internal-redistribution processes in the solid carbon for the time not longer than 100 ms [8].

Detailed investigations of fullerenes formation ways in flames were carried out by the group of Homann, studied the structure of a flame mainly by the direct introduction of ions and neutral particles into a mass spectrometer [9, 10, 12]. They investigated the premixed flames of acetylene [11], benzene [13], butadion and naphthalene with oxygen at a low pressure with the use of the molecular-beam sampling in combination with the mass-spectrometric analysis. It has been established that the bimolecular reaction between the PCAHs with a coordinated detachment of hydrogen, the so-called zipper mechanism, play an important role in the growth of fullerenes [11]. The reaction begins with the sandwich-like arrangement of two recondensed PCAHs (Fig. 2). A peculiarity of this reaction is that exactly 12 pentagons that are larger or equal to the coronene ($C_{24}H_{12}$) are formed in it independently to the PCAH size. At the same time, in accordance with the zipper mechanism, the pentagons should be transformed into the most appropriate energy state, *e.g.*, by the Stone-Wales method of pyracyclene redistribution [14].

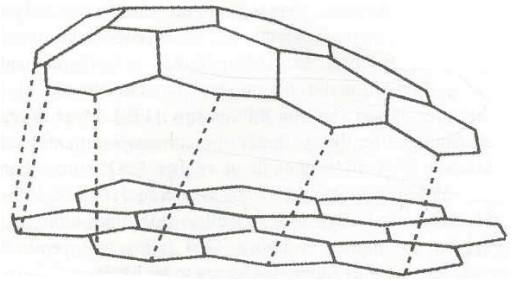

Fig.2. Model for the formation of five- and six-membered rings through the linkage of two PAHs by the zipper mechanism [11]

Formation of Fullerenes in the Combustion of a Benzene-Oxygen-Argon Mixture at a Low Pressure in an Electric Field

As is shown in [15], it is practically impossible to increase the yield of fullerenes in a combustion organized by the traditional method. In [16, 17], it was proposed to increase the fullerene yield by the action of an electric field on a flame. The authors of [18, 19] have shown that the synthesis of fullerenes formed in the plasma of an electric arc increase with increase in the electron density and in the ionization instability causing a change in the electron concentration from 1010 to 1011cm^{-3}. Despite the fact that the conditions of formation of fullerenes in a flame differ from those in an electric arc, these conditions are similar in their onset - the presence of the ionized initial products. An electric field applied to a flame changes the electron concentration and the flame temperature, with the result that the

conditions necessary for the formation of fullerenes are established.

A series of experiments on the study of the yield of fullerenes in a premixed benzene-argon-oxygen flame exposed to a longitudinal electric field under the conditions of a dark discharge, a corona discharge, and a glow discharge [16] at C/O=1.0, P = 40 torr, a benzene-flow rate Q_1 = 250 cm^3/min , an oxygen-flow rate Q_2 = 758 cm^3/min , an argon-flow rate Q_3 = 101 cm^3 (10% of the combustion-mixture volume), and a velocity of the cold mixture flowing from a perforated stabilizer V = 18.4 cm/c have been carried out [16]. Under these conditions, a steady-state combustion with a separation of the flame front from a burner $\delta = 0.5 \div 0.8$ cm was realized. The investigations were carried out in the voltage range 0.5-20 kV with electrode systems needle-plane and ring-plane at different interelectrode distances varying within the range 1-18 cm. The time of one experiment was τ = 20 min. After the experiment, the soot was gathered from the combustion chamber and from the filter of the soot collector and weighted; then the soot was extracted in benzene and investigated by physicochemical methods.

It has been established that the negative polarity of the upper electrode is more of favorable for the fullerene formation as compared to the positive one. However, in the experiments conducted at a negative polarity of the upper electrode under the conditions of dark, corona, and glow discharges at an interelectrode distance H = 18 cm with the use of a needle-plane system, a significant increase in the yield of fullerenes was not detected. At an interelectrode distance H = 18 cm, the upper electrode was positioned at a height of 10-11 cm above the upper edge of a flame. Under the indicated conditions, a discharge acted on the upper part of the flame, where a smaller number of ions are found [17-19] and the processes of formation of the output combustion products are practically absent. In this case, the calculated electron density did not exceed $\sim 10^5 \div 10^7$ cm^3. It has been established before that the optimum density of the free electrodes, providing a maximum yield of fullerenes, is $\sim 10^9$ cm^3. It is known [20] that, if the density of the charged particles in a gas is very small, they mainly interact with neutral particles. This interaction is short-lived, and the pair collisions are of first importance in such an ionized gas. When the density of the charged particles increases, the role of their interactions with each other increases gradually too. It is apparent that, under the above-described experimental conditions, the density of the charged particles is insufficient high to effectively influence the fullerene formation at an interelectrode distance of 18 cm.

The investigations carried out under the conditions where the upper electrode was positioned directly above a flame have shown that, in this case, the yield of fullerenes increases. The influence of the type of an electrode and the height of its position above a flame on the formation of fullerenes was investigated for determining the conditions providing their maximum yield. Electrodes in the form of a needle and a ring were used. The investigations were carried out at a negative polarity of the upper electrode under the conditions where UH =7 kV, H = 1-9 cm (with a step of 1 cm). A glow discharge appeared independently of the type of an electrode at different heights of its disposition above a flame; this discharge caused an intense glow of the whole flame (Fig. 3). In this case, the average temperature of the flame increased to T = 1200 °C (without a field, this temperature was equal to T = 950 °C).

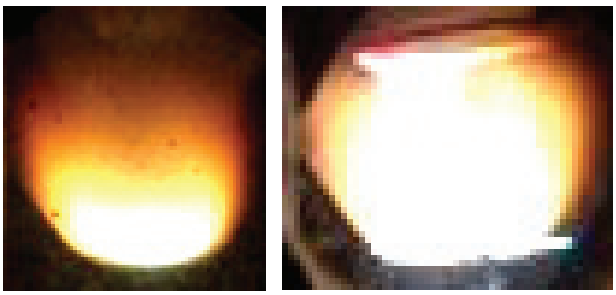

a b

Fig. 3. Action effect of glow discharge when positioning of ring form electrode on a central part of a flame: a – flame form without discharge, b – under discharge positioning ($U_н$ = 7 kW)

Thus, in the case where the upper electrode is placed directly above a flame, the near-cathode region of the glow discharge exerts a stronger influence on the processes occurring in the flame. An analysis of the soot extracts by the IR-spectroscopy method has shown that the fullerenes C60 (λ - 528, 577, 1183, 1429 cm^{-1}) with wavelengths lines with, corresponding to the fullerenes, are present in their spectra.

It has been established that a ring electrode offers an advantage over a needle one, and the largest yield of the C_{60} fullerene (β = 15% of the soot formed) was obtained in the case where it was positioned above the peripheral central part of the reaction zone of a flame (Table 1).

Table 1.
Influence of electric field on fullerenes formation under combustion of a benzene-oxygen-argon mixture

Experiments parameters	H = 6 cm I = 6,6 мА Uн = 7 kW		H = 4 cm I = 7 мА Uн = 7 kW		H = 6 cm I = 4,5 мА Uн = 12,5 kW	H = 4 cm I = 4 мА Uн=7 kW	H = 1 cm I = 3,8 мА Uн = 5 kW	Without field
Electrode form	Needle	Ring	Needle	Ring	Ring	Ring	Ring	-
Yield of soot, mg	0,5879	0,3825	0,3421	0,2245	0,4909	0,3623	0,5284	0,5958
Yield of soluble part, %	65,64	47,54	42,15	62,56	36,68	40,81	24,79	22,55
Yield of C60, %	5	13	10	15	2	5	<1	<1

The increase in the yield of fullerenes in the case where a ring electrode is placed above the peripheral part of the reaction zone of a flame is due to the glow-discharge conditions providing an effective synthesis of fullerenes. This statement is based on the results of the earlier investigations [13], showing that, if the peripheral zone of a benzene flame is heated by any external heat source, *e.g.*, a laser beam, which not simply burns the soot but forms the conditions identical to those at the center of the flame, the concentration of fullerenes increases.

The photographs of soot samples obtained with the use of a high-resolution JEM-3010 electron microscope of the JEOL firm with a magnifying power of up to 1,500,000 x at an accelerating voltage of 300 keV, show that these samples are highly structurized, which is characteristic of fullerene formations. It is known that the fullerenes formed in a flame are adsorbed, along with the polycyclic hydrocarbons, on the soot particles. The microscopic photographs of the soot samples are presented in Fig. 4 [21].

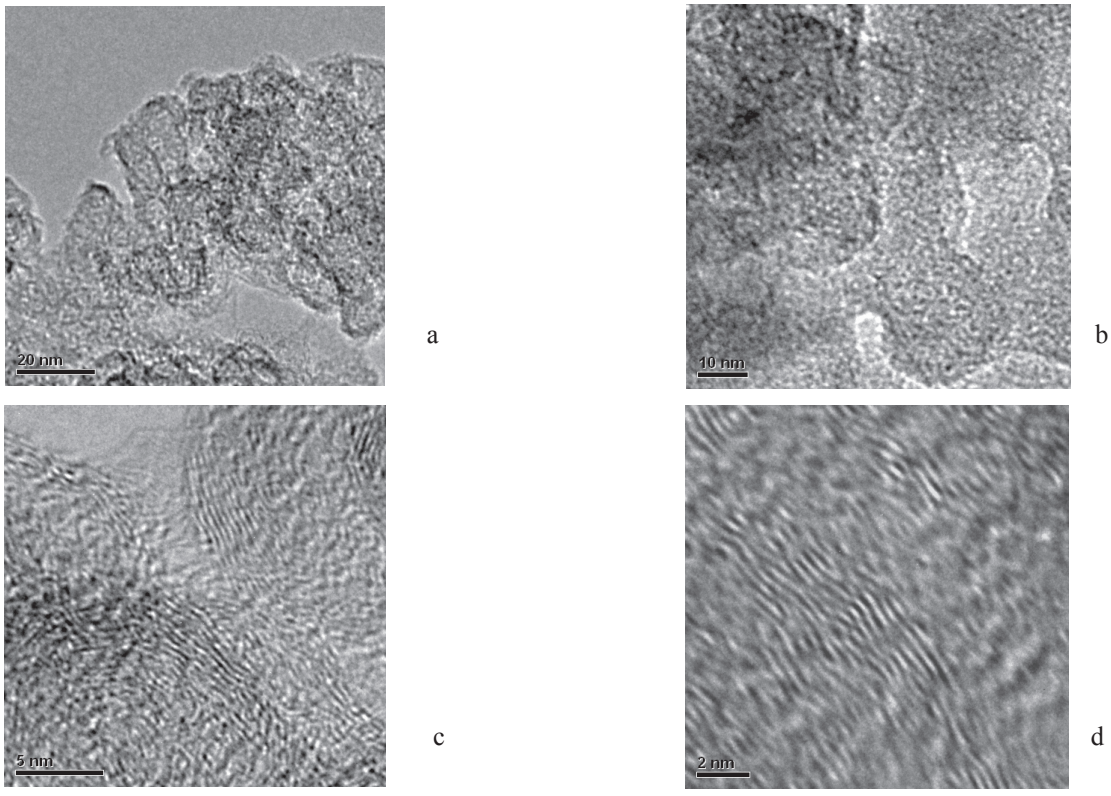

Fig. 4. Microscopic photographs of fullerene containing patterns of soot under different increasing

Table 2.
Results of fullerenes identification by their mass spectra

Stuff formula	Mass by estimation, а.м.u.	Mass by spectra, а.м.u.
C_{24}	288,26	288,3
$C_{16}H_{10}$ (pyrene, fluoranthene)	202,26	202,4
$C_{18}H_{10}$ (cyclopentepyrene, benzofluoranthene)	226,28	226,4
$C_{20}H_{10}$ (corannulene)	250,3	250,3
$C_{70}O$	856,77	856,7
$C_{70}H_2$	842,78	842,6
C_78	936,8	936,8
C_{94}	1129,03	1128,9
$C_{94}O$	1145,59	1145,5

The soot samples represent agglomerates consisting of spherical and nonspherical particles and amorphous soot (Fig. 4a). In this samples, spherical nanostructures with a diameter of up to 2 nm are also present (Fig. 4b). In (Fig. 4c), straight and bended carbon structures are seen. In the photographs obtained with a large magnifying power (Fig. 4d), one can see a layered carbonaceous material.

The benzene extracts of soot were investigated with the use of an ion-cyclotron-resonance Fourier spectrometer of the Bruker firm (of the type FT ICR MS Bruker «Apex Qe») with an electric-spray ionization. The mass-spectrometric investigations have shown that the fullerene oxides, $C_{60}O$, $C_{60}O_2$ $C_{60}O_3$ $C_{70}O$, $C_{94}O$ and as well as the higher fullerenes (C_{74}, C_{78}, C_{90}, C_{94}) are present in the indicated extracts [22]. The results of identification of fullerenes by their mass spectra are presented in Table 2.

Thus, it has been established that the yield of fullerenes increases under the action of a glow discharge in the case where an electrode (a needle or a ring) is positioned directly above flame and that a maximum yield of fullerenes is attained with the use of a ring electrode placed above the central region of the flame front. The maximum yield of the fullerene C_{60} was $\beta = 15\%$ of the soot formed.

Formation of Carbon Nanotubes and Nanofibers in Flames

In 1976, Endo observed the formation of carbon fibers in the pyrolysis of benzene [23] and, in 1991, Iijima detected carbon nanotubes in the graphite subjected to an arc discharge [24], which was the beginning of the era of carbon nanotubes that, due to their unique set of different properties are attractive materials from both the practical-application and fundamental-science standpoints [25, 26].

In a number of recent publications, results of the synthesis of carbon nanotubes in a flame used as a heat source, are presented. The production of carbon nanomaterials, such as nanotubes and nanofibers, in a flame has a number of advantages over the production of these materials with the use of electricity. First, in the case where a flame is used, here is no need to use an expensive electric heat source. Second, the flame synthesis, in point of fact, is simpler as compared to the synthesis with the use of electricity [27]. Yuan et al. [28] detected multiwall carbon nanotubes in the diffusion flames on a nickel-chrome wire and a stainless-steel net.

Van der Wal et al. [27] investigated the dependence of the structure of the carbon nanotubes formed in diffusion Cu, Fe, Ni flames on the Al_2O_3, CaO, SiO_2 and TiO_2 substrates with the use of Cu, Fe, and Ni as catalysts on the electron structure and chemical composition of these flames. They pointed to the fact that the electron interaction between the metal-catalyst particles and the supporting substrate substantially influences the density, homogeneity, and structure of the carbon nanotubes. Van der Wal et al. also used [29] a fuel-enriched premixed flame as a heat source and a thin-wire stainless-steel net covered with cobalt as a catalyst. The postflame gas

mixture was investigated with the use of different fuels is equal proportions for determining the optimum conditions for the growth of hydrocarbon nanotubes. They concluded that the molar fractions of approximately 0.105 for CO and H_2 are optimum, and such conditions can be realized with the use of an ethylene-air mixture in proportions 1.62.

Kennedy [30] has made a comprehensive survey of investigations on the synthesis of carbon nanotubes in the counterflow diffusion flames.

Savel'ev et al. [31] synthesized carbon nanotubes in the oxygen-enriched counterflow methane flames. The well-aligned nanotube bundles similar to bean-pods have been synthesized by Yuan et al. [32] with the use of a methane diffusion flame. Merchan-Merchan et al. [33] detected a thick layer of upright carbon nanotubes in the counterflow flame on the surface of a catalytic probe exposed to an electric field.

The typical temperature of the synthesis of carbon nanotubes and nanofibers in a diffusion flame with the use of catalytic methane is lower than the soot-formation temperature. The results obtained in [28-31] allow the conclusion that the formation of carbon nanotubes and nanofibers in a normal diffusion flame on a catalytic substrate takes place in the soot-formation zone of this flame. Unlike the diffusion flame, the formation of carbon nanotubes and nanofibers in any other flame on a catalytic substrate can take place outside the soot-formation zone beyond the flame front.

The flame synthesis of carbon nanomaterials is mainly determined by the carbon atoms serving as sources of graphite layers, the catalytic materials providing the fransformation of the gas-phase carbon atoms into the solid graphite layers, and the heat sources activating the catalytic metals. In [34], the synthesis of carbon nanotubes and nanofibers on a Ni $(NO_3)_2$ film deposited on a metal substrate with the use of a counterflow ethylene flame as a heat source was investigated.

Puri et al. have developed, on the basis of the numerous experimental data on the synthesis of carbon nanotubes in a flame, a model of formation of these nanotubes with the participation of the nanoparticles of catalysts (Fe, Ni, Co) [35, 36, 41]. In accordance with this model, the nucleation of carbon nanotubes begins when the density of the carbon atoms on the surface of the catalyst particles increases due to the addition of the indicated atoms from the outer shell of these particles. However, once the nucleation and growth of carbon nanotubes begin, carbon atoms are transported through nanoparticles mainly due to their diffusion that decreases with time because of the decrease in the concentration of the carbon atoms.

In Figure 5 the diagram of formation and growth in diffusion flame of carbon nanotubes on catalyst metallic nanoparticles has shown.

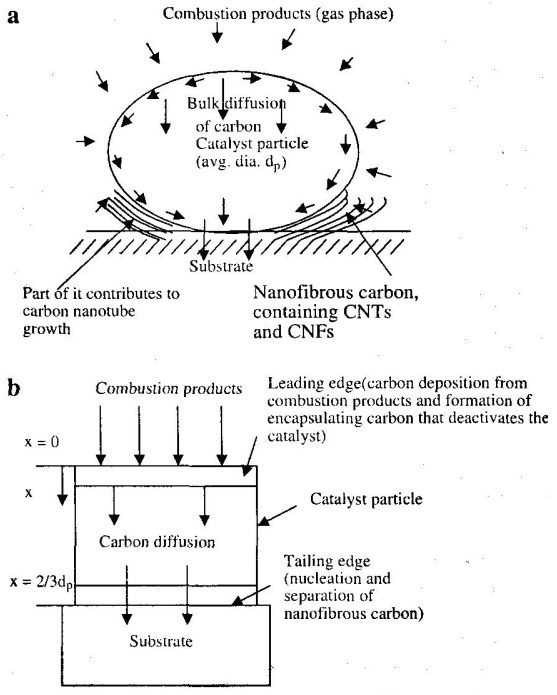

Fig. 5. Detailed model for flame synthesis of CNT and CNF [35]

The conditions of obtaining of different nano-particles in the counterflow propane-oxygen flames in a burner under different conditions of catalyst supply with the use of a Project ultrasonic atomizer were investigated in [37]. The aerosol formed in the ultrasonic atomizer was delivered through a hose pipe and a quartz tip to the flame-front zone. The consumption of the catalyst was determined by its weight before and after the experiment. The maximum flow rate of the catalytic solution was 0.9 cm3/min and its minimum flow rate was 0.3 cm^3/min. For the catalysts, $Fe(CO)_5$ and an alcohol solution ($Ni(NO_3)2*6H_2O$) were used. Alloy wire of diameter 0.7 mm was used as a substrate for growth of carbon nanotubes and metal nanoparticles. The regions of effective synthesis of nanomaterials in a counterflow flame were determined (Fig. 6).

Some of the samples obtained are presented in the electron-microscopic photographs. The metal particles obtained, shown in Fig. 7, have sizes from

30 to 70 nm. These particles were obtained in the «fuel zone» of a counterflow flame at a distance of 6 mm from its front in the process of atomization of the 20% alcohol solution $Ni(NO_3)_2 \cdot 6H_2O$ used as a catalyst; the characteristic temperature of the indicated zone is 400-500 °C.

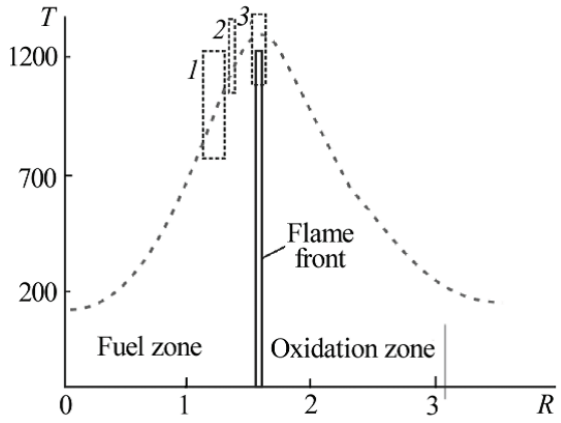

Fig. 6. Temperature profile showing three zones of nanomaterials formation on diffusional burner with counterjets [31]

Braids of carbon nanotubes have been detected in samples under the same conditions of combustion and catalyst-supply (Fig. 8). Figure 9 presents an electron-microscopic photograph of a sample obtained in a counterflow flame with the use of alloy wire of diameter 0.7 mm as a catalyst. The wire was positioned at a distance of 3 mm from the flame front in the «fuel zone» with a characteristic temperature of 1100-1200 °C.

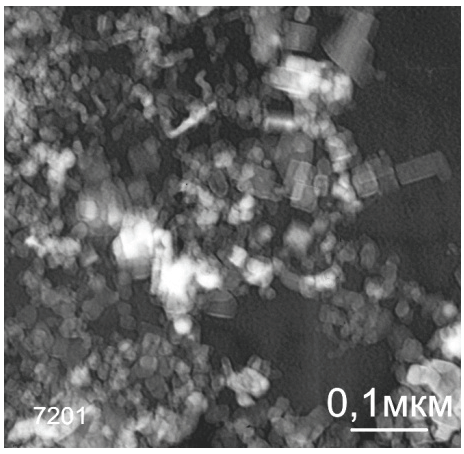

Fig. 7. Electron-microscopic photograph of a pattern with Ni particles.
Catalyst – 20% of alcohol solution $Ni(NO_3)_2 \cdot 6H_2O$ (aerosols)

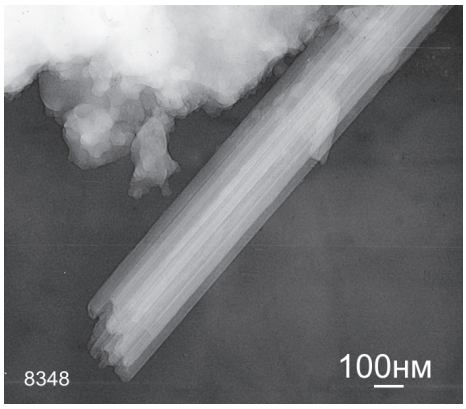

Fig. 8. Electron-microscopic photograph of pattern with carbon nanotubes tow. Catalyst – 20% of alcohol solution $Ni(NO_3)_2 \cdot 6H_2O$ (aerosols)

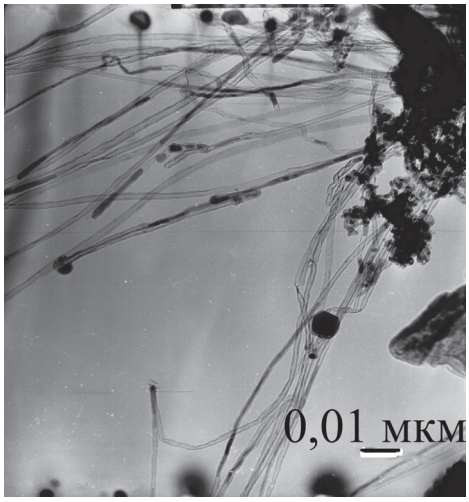

Fig. 9. Electron-microscopic photograph of a pattern. Catalyst – nichrome substrate.

Formation of Hydrophobic Soot in Hydrocarbon Flames

Low surface-energy materials like amorphous carbon (a-C) films [38] are frequently used to modify surfaces in order to control their wettability. Here, we present a technique for the rapid deposition of a superhydrophobic a-C layer consisting of uniform carbon nanobeads on a Si substrate using a coflow propane–oxigen nonpremixed flame [38]. The flame conditions have been described in detail previously [39]. The nanobeads are morphologically similar to the carbon nanopearls synthesized by Levesque and co-workers [40] through acetylene dissociation at 700 °C on nickel catalyst nanoclusters. Puri et al. have determined new ways of the synthesis of carbon nanotubes in the fuel-rich diffusion

flames, exposed to an electric field during 2-10 min, on superhydrophobic surfaces representing nanodimensional round amorphous carbon particles deposited on a silicon substrate [42, 43].

Surface hydrophobicity was determined by the angle θ between the solid surface and the tangent at the point of contact between the phases.

Energy retention drops on the surface is the product of the work of adhesion at the contact area $W_a S$. Tears drop of gravity $P = (\pi / 6) D_{\text{ė}}^3 \rho g$, where D_k - diameter of the drop, ρ - liquid density [44].

The purpose of this work is to determine the optimal conditions for formation of hydrophobic soot on substrates in the propane-oxygen flame and the effect of electric field on these processes, as well as to study the properties of the obtained products.

The formation of hydrophobic soot surface on silicon and nickel substrates during combustion of propane-oxygen flame was studied. The effect of electric field on these processes was studied and superhydrophobic soot surface with wetting angle θ > 170° was synthesized. It is stated that the hydrophobic properties are due to the presense of soot particles in the form nanobeads.

Modified combined burner was used for the synthesis of the hydrophobic soot in combustion of propane - oxygen mixture. Schematic diagram of the synthesis process is provided in Figure 10.

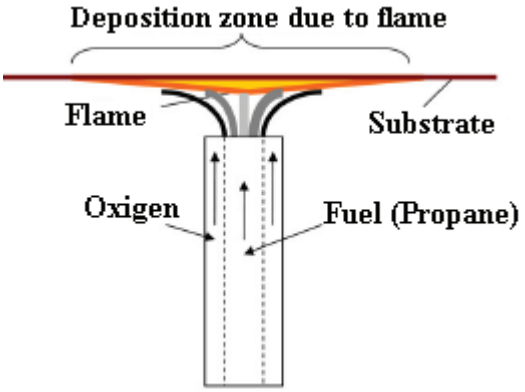

Fig. 10. Schematic diagram of the synthesis process

We varied the distance from the matrix burner and the substrate, the exposure time, and investigated the influence of an electric field. Changed the polarity and magnitude of the applied voltage.

The formation of the hydrophobic soot surface on silicon substrates and nickel during combustion of propane - oxygen flame. In Figure 11 shows a photograph of the experimental device.

Fig. 11. Photograph of the experimental device

The temperature gradient in the volume of the flame plays an important role in the formation of soot particles. Cost ratio of combustible mixture composes: 50 cm^3/min propane, oxygen, 260 cm^3/min. Flame visual can be divided into two zones. Lower - blue zone, which becomes yellow - red zone. The height of the blue zone is about 0.5 cm with a temperature of 770 K. At the distance of 1 to 2 cm, a sharp rise in temperature, from 2 to 2.5 cm observed relative stabilization, then, from 2.5 cm a further rise in temperature and its maximum value of 1470 K is reached at a distance of 4 cm above there is a gradual decline in temperature. Stabilization of the temperature from 2 to 2.5 cm is due to the heat capacity of the formed soot particles, which stores the heat, that is, at a height of 2 cm from the start of the flame front starts copious soot formation.

Time of exposure to flame ranged from 4 to 10 min. When the exposure time of less than 4 minutes on the substrate ordinary soot is deposited. Exposure time of more than 4 minutes lead to the formation of soot with hydrophobic properties and the separation of the resulting surface area. Figure 12 shows a sample obtained using a silicon substrate, the surface is visually possible to observe the separation of soot settled on the three zones.

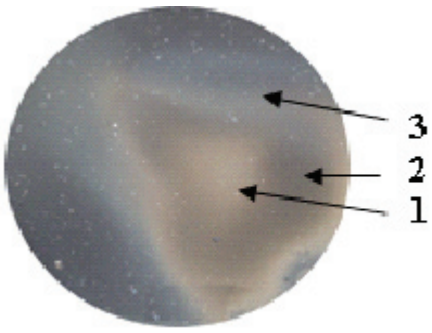

Fig. 12. Silicon disc, which was exposed to a flame

Zonal deposition of soot particles on the surface of the silicon substrate due to the fact that in different areas of the flame generated soot particles with different properties.

To determine the morphology and size of soot particles formed on the substrates were carried out electron microscopic studies of the samples. Figure 13 shows electron micrographs of two samples of soot on the substrates, which are manifested as hydrophobic properties, and there is a clear division into zones. The nanostructured coatings consisted of similarly agglomerated solid particles or nanobeads. Their deposition occurred during combustion through gas phase fuel pyrolysis in the oxygen-deficient flame core. In this core, heavier hydrocarbons were transported into the stagnation layer adjacent to the relatively colder substratum surface and condensed upon it to form the nanostructures.

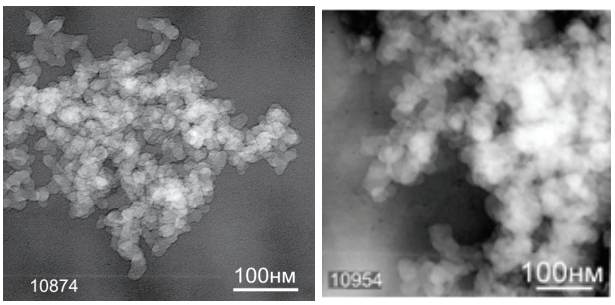

Without applying an electric field | With an electric field

Fig. 13. Electron morphostructures

Soot surface was synthesized according to the proposed method in this paper. Sample 1 was obtained on a silicon substrate at a rate of 260 cm^3/min oxygen, propane, 50 cm^3/min, the height above the burner plate 2 cm, exposure time 10 min without applying an electric field, and sample 2 with an electric field of negative polarity with a magnitude of voltage 1 kV, other conditions are identical to a sample. Studies have shown that carbon deposits on the plates are differences in the morphological structure of deposited particles in different zones. In the central and middle zone formed long chains of individuals in the form nanobeads 15-30 nm without applying an electric field, and 40-50 nm when an electric field. In the outer zone, regardless of the conditions of combustion, there are coagulated aggregates of soot particles with sizes 30 - 50 nm.

The degree of hydrophobic surface is characterized by wetting angle: for hydrophilic surfaces $\theta<900$, for hydrophobic surfaces $\theta>900$. Measured by sessile drop method. This method was applied to determine the hydrophobicity of the obtained soot surface, using photographs. Below are photos of applying a drop of water on a clean silicon surface, as well as in three zones of the resulting soot surface on a silicon substrate. It is seen that a water droplet deposited on a clean silicon surface has an external contact angle 50°, ie, surface exhibits hydrophilic properties (Figure 14, a). Figures 14 (b, c, d) shows photographs of droplets deposited in the central gray zone, middle zone of brown and black outer zone (Figure 12). Contact angle is the gray area - 135°, brown band - 155° and external black zone - 145°. The data obtained shows that the soot settled in the middle brown band, has the best hydrophobic properties compared with soot, settled in the central and outer zones.

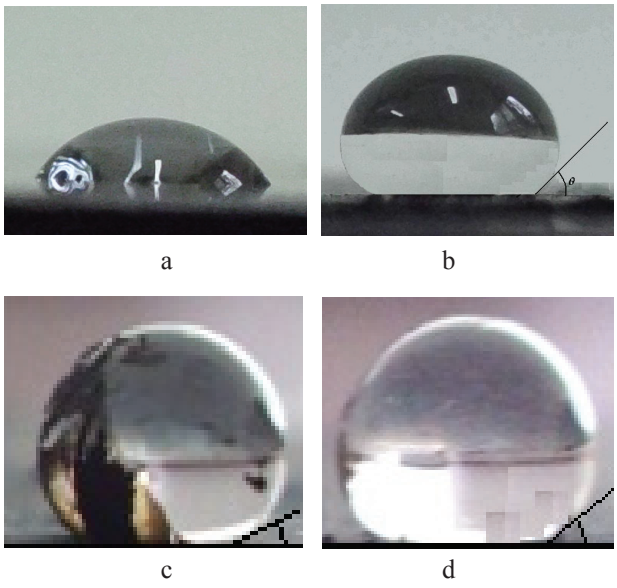

Fig. 14. A drop of liquid on the hydrophilic (a) and hydrophobic (b, c), and superhydrophobic surface (d)

When applying strong electric fields on flames, due to collisions of fast electrons, in addition there are excited molecules, molecular ions or the dissociation of molecules into neutral ionized fragments (atoms, radicals). Excited state of such particles is metastable, thus they are relatively long-lived and the combustion process in this case is somewhat different from the combustion under normal conditions. To determine the effect of external influence on the hydrophobic properties of the resulting carbon black surfaces have conducted studies with the imposition of the flame of the

electric field. The experiments were performed on silicon substrates, and nickel at low values of imposed stress and strain over 500 volts when the imposed electric field enters the discharge.

When a voltage of 1 kV and over the flames visually changing, it becomes brighter, there is a periodic jumping spark and there is plenty of soot formation, which in large quantities is deposited on the substrate in the form of dendrites. Without applying an electric field the flame spreads over the surface of the substrate. With an electric field the flame propagates in the form of a cylinder with a diameter of 1.5 cm up to touch the substrate. This phenomenon is vividly expressed in the imposition of a negative polarity on the substrate, while the flame adheres to it. With positive polarity appears small gap between the upper front «of the flame and the substrate.

In the long process of flame electric field, passing in the discharge, there is an increase soot of the entire space between the die and substrate. Current increases to 700 μA . Application of an electric field in the discharge increases the thickness of the carbon of the hydrophobic layer and narrowing of the spread. Regardless of the substrate material, the magnitude and polarity of the imposed stress, observed the same dependence of the properties received by the surface. In the middle part of the substrate, diameter 2,5 - 3 cm, the soot formation of superhydrophobic surface with a wetting angle above (Figure 15). Closer to the edge of the substrate, a sharp transition of hydrophobic soot to hydrophilic (Figure 16).

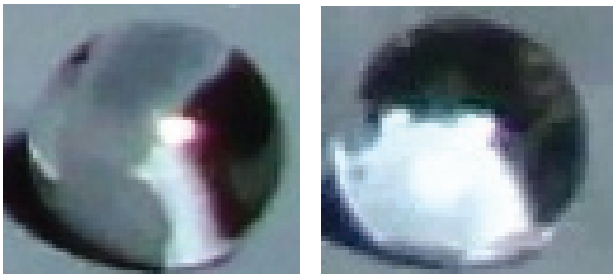

Fig. 15. Superhydrophobic surface of the soot obtained by applying an electric field

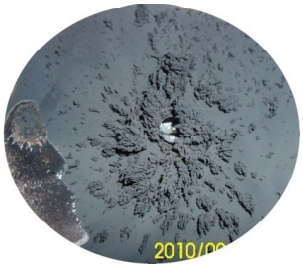

Fig. 16. Transition of hydrophobic soot to hydrophilic

The study of the conditions of interaction of surfactants with the resulting hydrophobic soot surface on a silicon substrate. Studied the modifying effect of anionic - sodium dodecyl sulfate ($C_{12}H_{25}OSO_3$ Na), cationic - tsetilperidiniya bromide ($C_{16}H_{33}C_5H_5N$ Br) and a nonionic surfactant - alkylphenol oxyethylenated ($C_{16}H_{33}C_6H_4O(CH_2CH_2O)_{10}H$). Studies have shown that the contact angle is the soot surface water is 150° - this confirms the superhydrophobic surface properties. For comparison, we note that such hydrophobic surface like teflon has angle of wetting 105 - 110°. When wetting the carbon surface in the presence of surfactants of different nature is established that when the surfactant concentration from 10^{-5} to 10^{-1}, a change in surface properties from hydrophobic to hydrophilic. In this case, ionic surfactants have a greater modifying effect than nonionic surfactants. The difference in the modifying effect of ionic and nonionic surfactants due to the difference in the degree of hydration of polar groups of surfactants. Based on the values of the surface tension of surfactants and wetting angles were determined the values of adhesion energy and plot the work of wetting of the logarithm of concentration (Figure 17).

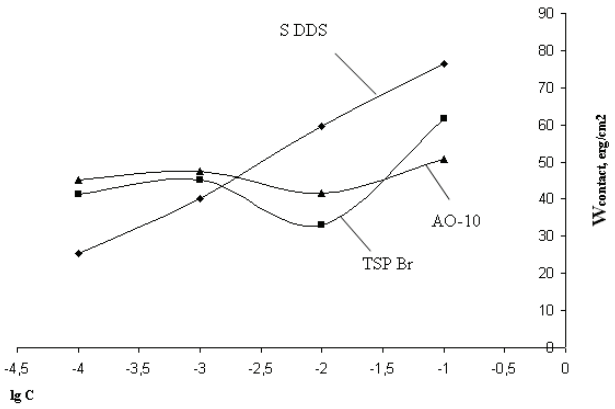

Fig. 17. Dependence of the wetting of the logarithm of the concentration

The results showed that the greatest work of wetting is found for sodium dodecyl sulfate (SDS Na). Thus, modifying sooting surface using surfactants of different nature, we can achieve the necessary degree of hydrophilicity, which can be used for targeted regulation of hydrophobicity obtained soot surfaces. This may find application in nanotechnology, in preparation hemosorbents, biosensors, etc.

Conclusion

It was established the formation of fullerenes and carbon nanotubes as well as soot with the superhydrophobic surface, obtained on nickel and silicon supports in benzene-oxygen and propane-oxygen diffusion flames. New results regarding the synthesis of superhydrophobic surface with a contact angle 135-175° have great practical interest as anti-corrosion additives to various materials.

References

1. Kroto H.W., Heath J.R., O'Brien S.C., et al. C60: Buckminsterfullerene // J. Nature 1985, V. 318. P.162-163.
2. Fullerens and Related Structures / Ed. A. Hirsh Berlin; Springer. 1999.
3. Gerhardt P., Loffler S., Homann K.H. The formation of polyhedral carbon ions in fuel-rich acetylene and benzene flames // 22 Symp. (Intern.) on Combustion. Pittsburgh: The Combustion Inst., 1988. P. 395-401.
4. Howard J.B., McKinnon J.T., Makarovsky Y., et al. Fullerenes C60 and C70 in flames // Nature 1991, V. 352. P. 139-141.
5. Howard J.B., Lafleur A.L., Makarovsky Y., Mitra S., Pope C.J., Yadav T.K. Fullerenes synthesis in combustion. Carbon 1992;30.1183-201.
6. Richter H., Labrocca A.J., Grieco W.J., Taghizadeh K., Lafleur A.L., Howard J.B. Generation of higher fullerenes in flames. J Phys Chem B 1997;101:1556-1560.
7. Chowdhury K.D., Howard J.B., Vander Sande J.B. Fullerenic nanostructures in flames. J Mater Res 1996; 11:341-7.
8. Howard J.B. Fullerenes formatiom in flames // 24nd Symp. (Intern.) on Combustion. Pittsburgh: The Combustion Inst., 1992. P. 933-946.
9. Bachmann M., Wiese W., Homann K-H. Thermal and Chemical influences on the soot mass growth // 25 th Symp. (Intern.) on Combustion. Pittsburgh: The Combustion Inst., 1994. P. 635-643.
10. Ahrens J., Kovacs R., Shafranovskii E.A., Homann K-H. Online multi-photon ionization mass spectrometry applied to PAH and fullerenes in flames. Rer Bunsenges Phys Chem 1994;98:265-268.
11. Ahrens J., Bachmann M., Baum T., Griesheimer J., Kovacs R., Weilmunster P., Homann K-H. Fullerenes and their ions in hydrocarbon flames. Int J Mass Spectrom Ion Process 1994;138:133-48.
12. Bachmann M., Wiese W., Homann K.-H. Fullerenes versus soot in benzene flames // Combust. Flame. 1995. V. 101. P. 548-550.
13. Bachmann M., Wiese W., Homann K-H. PAH and aromers: precursors of fullerenes and soot. Twenty-sixth Symposium (International) on Combustion, The Combustion Institute. Pittsburgh. 1996. p. 2259-2267.
14. Stone A.J., Wales D.J. Theoretical studies of icosahedral C60 and some related species. Chem Phys Lett 1986;128:501-503.
15. Zolotukhin I.V., Gustov A.V. Analize metodov polucheniya fullerenov // Perspektivnye materialy. – 2002. - № 2. – C. 5-12.
16. Mansurov Z.A., Prikhodko N.G., Mashan T.T., Lesbaev B.T. Formation of PAN, Fullerences, Nanoparticles and Soot at Combustion of hydrocarbons in Electric Field. Proceedings of the 20th International Colloquium on the Dynamics of Reactive Systems, 2005, July 31-August 5, Montreal, Canada. CD, p.5.
17. Stepanov E.M., D'yachkov B.G. Ionizaciya v plameni i electricheskoe pole. - M.: Metallurgiya, 1968. - 312 p.
18. Lauton G., Vainberg F. Electricheskie aspecty goreniya / Transl.from Engl.; editor V.A. Popova - M.: Energiya, 1976. - 296 p.
19. Calcote H. F., Gill R.J. Comparison of the Ionic Mechanism of Soot Formation with a Free Radical Mechanism // Soot Formation in Combustion. Mechanisms and Models / Ed. H. Bockhorn. Springer Series in Chemical Physics. - Berlin: Springer, 1994. - Vol. 59. - P. 471-484.
20. Rayzer Y.P. Fizika gazovogo razryada. - M.: Nauka, 1987. - 590 p.
21. Mansurov Z.A., Prikhodko N.G., Lesbaev B.T., Mashan T.T. Combustion of the Premixed Benzene-Oxygen Mixture in Electric Field at Low Pressure // 31st International Symposium on Combustion. - Heidelberg, 2006. - P. 164.
22. Mansurov Z.A., Lesbaev B.T., Chenchik D.I., et. al. Synthesis of Fullerenes and Carbon Nanotubes in Flames // Book of abstracts. Inter. Conf. on Carbon. - Nagano, 2008. - P. 134-139.
23. A. Oberlin, M. Endo, T. Koyama: Filamentous growth of carbon through benzene decomposition, J. Cryst. Growth 32, 335-349 (1976).

24. S. Iijima: Helical microtubules of graphitic carbon, Nature 354, 56-58 (1991).
25. Morinobu Endo. Potential Applications of Carbon Nanotubes: Topics in applied physics, Springer-Verlag Berlin Heidelberg – 2008. – 13-61 P.
26. Z.A. Mansurov. Some applications of nanocarbon materials for novel devices / R. Gross et. al (eds.), Nanoscale Devices - Fundamentals and Applications, 355-368. 2006 Springer.
27. R.L. Vander Wal, T.M. Ticich, V.E. Curtis. Substrate–support interactions in metal-catalyzed carbon nanofiber growth // Carbon 39 (2001) 2277-2289.
28. L. Yuan, K. Saito, W. Hu, Z. Chen. Ethylene flame synthesis of well-aligned multiwalled carbon nanotubes. // Chem. Phys. Lett., 2001, V. 346, p. 8.
29. R. L. Vander Wal, L.J. Hall, G.M. Berger Optimization of Flame Synthesis for Carbon Nanotubes Using Supported Catalyst // J. Phys. Chem. B, 2002, 106 (51), pp 13122–13132.
30. Kennedy L.A. Carbon nanotubes, synthesis and orientation control in opposed flow diffusion flames. J. oh Heat Transfer-Transactions of the ASME. 2008. 130 (4).
31. Saveliev W., Merchan-Merchan. L.A. Kennedy. Metal catalyzed synthesis of carbon nanostructures in an opposed flow methane oxygen flame // Combust. Flame 135 (2003) 27-33.
32. L. Yuan, T. Li, K. Sano. Synthesis of multiwalled carbon nanotubes using methane/air diffusion flames // Proc. Combust. Inst. 29 (2002) 1087-1092.
33. W. Merchan-Merchan. A.V. Saveliev, L.A. Kennedy. High-rate flame synthesis of vertically aligned carbon nanotubes using electric field control // Carbon 42 (2004) 599-608.
34. G.W. Lee, J. Jurng, J. Hwang. J. Formation of Ni-catalyzed multiwalled carbon nanotubes and nanofibers on a substrate using an ethylene inverse diffusion flame // Combust. Flame 139 (2004) 167-175.
35. S. Naha, S. Sen, A. K. De, I.K. Puri. A detailed model for the flame synthesis of carbon nanotubes and nanofibers // Proceedings of the Combustion Institute, Volume 31, Issue 2, (2007), P. 1821-1829.
36. S. Naha, I.K. Puri. A model for catalytic growth of carbon nanotubes // J. Phys. D: Appl. Phys. 41 (2008) 065304 (6 pp).
37. Mansurov Z.A., Prikhodko N.G., Lesbaev B.T., Chenchik D.I. Control of the synthesis of fullerenes and nanotubes in hydrocarbon flames // Bock of abstracts. First Asian carbon conference. – Delhi, (2009). – P. 9.
38. Robertson J. Diamond-like amorphous carbon. Mater Sci Eng R 2002; 37 (4 - 6): 129 - 281.
39. Sen S, Puri IK. Flame synthesis of carbon nanofibers and nanofiber composites containing encapsulated metal particles. Nanotechnology 2004; 15 (3): 264 - 8.
40. Levesque A, Binh VT, Semet V, Guillot D, Fillit RY, Brookes MD, et al. Mono disperse carbon nanopearls in a foam-like arrangement: a new carbon nano-compound for cold cathodes. Thin Solid Films 2004; 464-465: 308 - 14.
41. S. Naha, S. Sen, I.K. Puri. Flame synthesis of superhydrophobic amorphous carbon surfaces // J. Carbon V. 45, Issue 8, (2007), P. 1702-1706.
42. S. Mazumder, S. Ghosh, I. Puri. Nonpremixed flame synthesis of hydrophobic carbon nanostructured surfaces // 33 th. Symp. (Intern.) on Combustion. Pittsburgh: The Combustion Inst., (2010).
43. S. Banerjee, S. Naha, I.K. Puri. Molecular simulation of the carbon nanotube growth mode during catalytic synthesis // Appl. Physics Letters 92, 233121 (2008).
44. Komissarov A.V. This article draws from the portal «NANO NEWS NET» http: //www. nanonewsnet.ru.

Received 9 June 2010.